Zeitschrift: Bulletin des Schweizerischen Elektrotechnischen Vereins

Herausgeber: Schweizerischer Elektrotechnischer Verein ; Verband Schweizerischer Elektrizitätswerke

Band: 51 (1960)

Heft: 20

Artikel: Parametric Circuits at Low Frequencies Using Ferrites and Thin Magnetic Films

Autor: Brändli, A.

DOI: https://doi.org/10.5169/seals-917074

Betriebsdaten von Klystron Nr. 6

Tabelle VIb

Betriebsdaten			
Benennung	Symbol	Einheit	Daten
Betriebsspannung	U_0	kV	1,6
normierte Strahlgeschwindigkeit	$\beta = \frac{v_0}{c}$	—	0,079
Teilwellenkonstante	$\frac{1}{A^2}\Sigma f_k^2$	—	0,495
Strahlbelastung	G_B	$1/\Omega \cdot 10^{-6}$	3,0
elektronische Steilheit	S_e	$1/\Omega \cdot 10^{-4}$	keine Angaben
Strahlbelastung nach Derfler	G	$1/\Omega \cdot 10^{-6}$	2,35
elektronische Verstimmung nach Derfler	B	$1/\Omega \cdot 10^{-6}$	3,42
elektronische Steilheit nach Derfler	K	$1/\Omega \cdot 10^{-4}$	1,43
experimentelle Verstärkung	v_{exp}	db	81,6
theoretische Verstärkung nach Feenberg	$v_{th}\,F$	db	81,2
theoretische Verstärkung nach Ramo	$v_{th}\,R$	db	84,8
Verstärkung nach Derfler	v_D	db	81,9

Zusammenfassung

Die Röhren Nr. 1...3 zeigen einen sehr grossen Unterschied zwischen theoretischer und experimenteller Verstärkung, während bei den Klystrons 4...6 die Übereinstimmung zwischen Theorie und Experiment sehr gut ist.

Der Grund für die Diskrepanz bei den ersten drei Röhren kann nur vermutet werden. Die Derflersche Theorie nimmt an, dass dem Strahl am Eingangsspalt die Modulationsleistung von einer starken Quelle aufgedrückt werde. Da über die experimentelle Anordnung in den Literaturstellen nichts ausgesagt worden ist, bleibt die Frage offen, ob die gesamte gemessene Eingangsleistung wirklich zur Strahlmodulation verwendet wird. Die Vermutung, dass dies nicht der Fall ist, liegt nahe, da die gemessene Verstärkung kleiner war als die von der Theorie verlangte. Ein anderer Grund könnte in einer falschen Abschätzung des belasteten Resonatorwiderstandes liegen, schliesslich wäre es denkbar, dass die Derflersche Theorie, die für Klystrons mit mehr als zwei Resonatoren bessere Resultate liefert als für Zweikreis-Röhren, noch einer Korrektur bedarf, welche eine u. U. zwischen Ausgangsresonatorspalt und Auffängerelektrode vorliegende stehende Welle und ihren Einfluss auf die Spannung über dem Ausgangsspalt berücksichtigt.

Literatur

[1] *Hamilton, D. R., J. K. Knipp* und *J. B. Horner Kuper:* Klystrons and Microwave Triodes. MIT Radiation Laboratory Series Bd. 7. New York: McGraw-Hill 1948.

[2] *Beck, A. H. W.:* Velocity-Modulated Thermionic Tubes. Cambridge: Univ. Press 1948.
Beck, A. H. W.: Space-Charge Waves and Slow Electromagnetic Waves. London: Pergamon 1958.

[3] *Derfler, H.:* Zur Theorie der Elektronenstrahlröhren mit periodischem Aufbau. Mitt. aus dem Inst. für Hochfrequenztechnik an der ETH in Zürich, Nr. 19. Zürich: Leemann 1954.

[4] *Madelung, E.:* Die mathematischen Methoden des Physikers. 5. Aufl. Berlin: Springer 1953. S. 109.

[5] *Beck, A. H. W.:* Space-Charge Waves and Slow Electromagnetic Waves. London: Pergamon 1958.

[6] *Derfler, H.:* Plasma-Waves in Finite Electron Beams and their Interaction with Field Waves. Travaux du Congrès International «Tubes Hyperfréquences», Paris, 29. Mai bis 2. Juni 1956. Vortrag 4.1.01. Bd. 1, S. 326...336.

[7] *Lawson, J. D., R. S. Barton, T. F. Gubbins, W. Millar und P. S. Rogers:* The Design and Performance of a High Power Demountable Klystron Amplifier for X-Band. J. Electronics Bd. 1 (1955/56), Nr. 3, S. 333...354.

[8] *Cockroft, H. S.* und *J. R. Pickin:* X-Band Klystrons for High Power C. W. Operation. J. Electronics Bd. 1(1955/56), Nr. 4, S. 359...372.

[9] *Chalk, G. O., B. W. Manley* und *V. J. Norris:* A Five Cavity X-Band Klystron Amplifier. J. Electronics Bd. 2(1956/57), Nr. 1, S. 50...64.

[10] *Newton, R. H. C., B. B. Dyott, W. H. Aldons* und *W. E. Rowlands:* A High Power X-Band CW Klystron Amplifier. Travaux du Congrès International «Tubes Hyperfréquences», Paris, 29. Mai bis 2. Juni 1956. Vortrag 3.02. Bd. 1, S. 247...261.

Adresse des Autors:
H. Hagger, Dipl. Ingenieur, Institut für Hochfrequenztechnik an der ETH, Sternwartstrasse 7, Zürich 6.

Parametric Circuits at Low Frequencies Using Ferrites and Thin Magnetic Films

By *A. Brändli*, Syracuse

621.375.9.029.6+621.314.26+621.373

1. Introduction

In recent years parametric devices have received considerable attention. This is particularly true of the voltage-controlled capacitance in the form of the back-biased semiconductor diode since it permits low noise amplification at high frequencies. Parametric operation can also be obtained with a variable inductance device such as a coil wound on ferrite material having a nonlinear *B-H* characteristic. The main advantage of ferrites over diodes is their greater immunity to nuclear radiation [1; 2][1]). This property is important in applications associated with space vehicles, etc.

Other applications of nonlinear ferrites are in the computer area, where ferrite devices (such as the "parametron") are used as parametric subharmonic oscillators.

At the present time work is being done in the field of thin magnetic films. Due to the special method of deposition, namely in the presence of a dc magnetic field, these films show anistropic properties which make them suitable for applications in the parametric area. The frequency limit of operation is expected to be in the UHF region.

2. Parametric Operation and Related Circuits

2.1 Parametric Operation in general

In order to obtain parametric operation, namely subharmonic oscillation or frequency conversion or amplification,

[1]) Refer to the Bibliography at the end of the article.

based on a variable inductance, a magnetic material is needed which exhibits a nonlinear *B-H* characteristic as shown in Fig. 1. The small signal inductance, the derivative of the above characteristic, is represented in the same figure. If the material is biased at a point P and a sufficiently large pump signal is applied, an inductance change is produced which is most pronounced at the pump frequency. As a consequence, parametric operation is possible. A simplified analytical treatment is shown in Appendix 1.

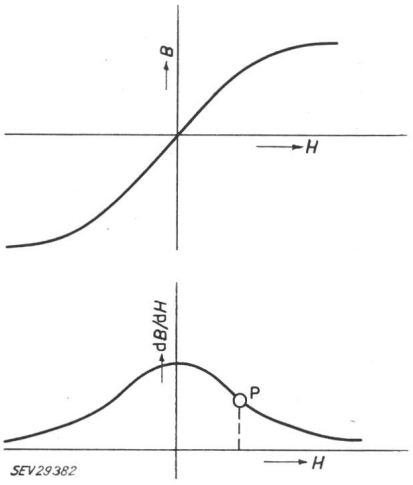

Fig. 1

Nonlinear magnetic characteristic and small signal inductance

For coil with one turn
B Magnetic induction; *H* Field-strength
(For explanation of point P refer to text)

Depending upon the frequency relationship which is established between the input frequency f_1, the output frequency f_2 and the pump frequency f_0 by suitable filters, the following circuit types can be distinguished:

		Gain
$f_1 + f_0 = f_2$ noninverting[2]) case	$f_1 < f_2$ up converter	$\frac{f_2}{f_1} > 1$
	$f_1 > f_2$ down converter	$\frac{f_2}{f_1} < 1$
$f_1 + f_2 = f_0$ inverting[2]) case	$f_1 < f_2$ up converter $f_1 > f_2$ down converter input *and* output at same frequency: amplifier[3])	any value depends on pump power

2.2 *Circuits using cores*

In order to avoid any interference between the large pump signal on the one hand and the usually small input and output signals on the other, a circuit with two cores is used on which the pump windings are in opposition to the input and output windings as shown in Fig. 2. Further filtering is achieved by the tuned circuits.

[2]) The name "inverting" means that a positive change δf_1 of f_1 is inverted resulting in a negative change $\delta f_2 = -\delta f_1$ because of the frequency relation $f_1 + f_2 = f_0$.

[3]) The amplifier is a two-terminal device which utilizes the negative input resistance of the inverting converter at the frequency f_1 (or f_2). The tank circuit at the frequency f_2 (or f_1), called the idler circuit, is necessary for parametric operation although it is not used as an output.

A partial transmission of input energy at the frequency f_1 into the output circuit and vice versa still takes place due to the transformer action of the cores. A partial compensation can be achieved by a four-core circuit (see Fig. 3) in which only two cores are driven by the pump and the other two just act as compensating transformers. The dc bias is the same for all cores. A more careful consideration shows that the compensation is not complete, not only from a practical but also from a theoretical point of view.

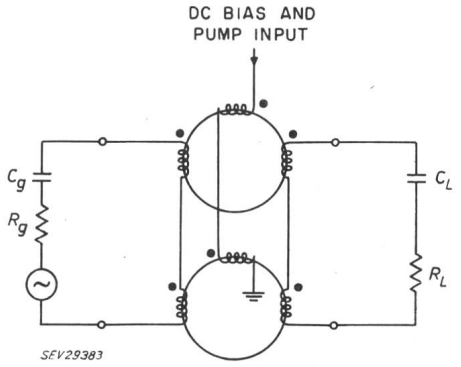

Fig. 2

Two-core circuit separates pump from input and output

The generator impedance (C_g, R_g) and the load impedance (C_L, R_L) are tuned to the input and output frequencies with the input and output inductances respectively.

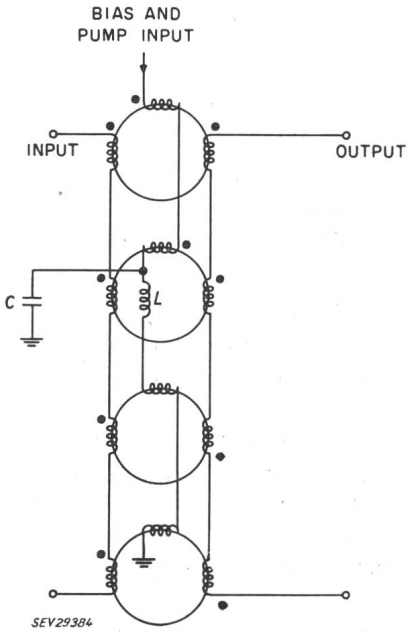

Fig. 3

Four-core circuit

C By-pass capacitor; *L* Choke

A circuit which separates each signal from the others in a rigorous way is the bridge shown in Fig. 4. It consists of four equal cores having two windings each. The "inside" windings serve to apply the dc bias and the pump; the "outside" windings are part of the input and output circuit. The operation of the circuit is described in detail in Appendix 2. However, by simple inspection it can be seen that:

a) there is no interference between the pump and the input signal because of the reversed polarity of the transformers 1 and 3 on one side and 4 and 2 on the other;

b) similarly there is no interference between the pump and the output signal since the transformers 1 and 4 and correspondingly 3 and 2 are fed by the pump in antiphase with respect to the output;

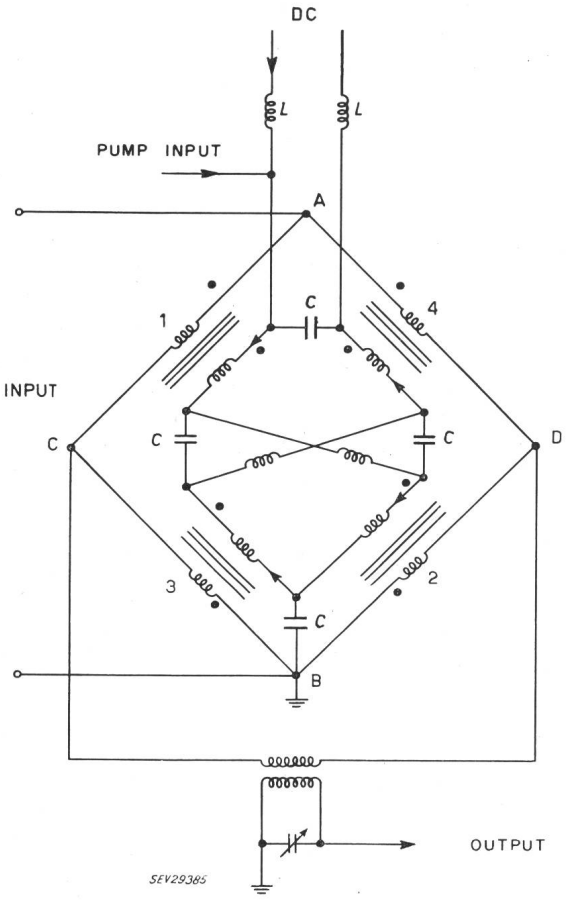

Fig. 4
Bridge type parametric circuit
L Choke; *C* By-pass capacitor

c) there is no transmission by transformer action of signal at the frequency f_1 to the output since the circuit is a bridge. For the same reason, no signal at the frequency f_2 appears at the input.

For these reasons the output signal is free from interference and is due purely to the parametric conversion process. In a practical circuit only an approximate balance can be obtained. It is therefore advisable to tune each circuit to the appropriate frequency thereby improving the separation.

It may be seen that in Fig. 4 the transformers are fed in series dc-wise but in parallel (two by two) ac-wise. Consequently at a particular instant of time the inductances No. 1 and 2 will increase, while No. 3 and 4 decrease. This is necessary in order to obtain any output at all (see Appendix 2 for details) because, if all the transformers were in the same condition at every instant of time, no conversion would take place.

2.3 Magnetic films

2.3.1 General

During the past few years a considerable amount of work has been done in the area of thin magnetic films. These films are vacuum evaporated or electro-deposited, on a glass plate for example, to a thickness of 10 ... 10^4 Å (10^{-3} ... 10 μm) in the presence of a dc magnetic field. As a result, the film is magnetized in the field direction, the so called "easy direction of magnetization." As an external field is applied the magnetization vector is rotated to include an angle φ with the easy direction (Fig. 15). As a consequence the film's free energy, which is a function of the field and φ, assumes a minimum value, thereby determining the angle φ. Thus the static behavior of the film (*B-H* characteristic for different directions, etc.) is determined, as shown in Appendix 3.

In order to apply or detect the magnetic fields parallel and perpendicular to the easy axis, appropriate coils perpendicular to each other can be used. The analysis shows that the small signal inductance of each coil depends mutually on the current through the other coil, but in principle no transformer coupling exists between them since their axes are perpendicular.

2.3.2 Applications

An important application of thin magnetic films is as bistable memory elements in digital computers. Here the main advantages of films over cores are the greatly reduced switching time (for example, 10 ns instead of 1μs for cores) and the potentially simple fabrication.

Another application lies in the parametric area, where films can be used either as subharmonic oscillators (representing the information "0" or "1" by the phase 0 or π of the oscillator) or in CW-applications as parametric amplifiers and converters. It is expected that films will operate up to the UHF region. The power level of the signal in a thin film device depends on the area and thickness and is rather low, in the order of microwatts, for a film of 1000 Å (10^{-4}) thickness on a 0.1 inch square plate (2.5 × 2.5 mm).

As far as immunity against nuclear radiation is concerned no specific information on films is available, but figures similar to those found with thicker Ni-Fe samples are expected [2].

A problem from the circuit point of view is to obtain sufficiently tight coupling between the fields within the thin film and the currents flowing in associated circuit elements. In memory applications this is important for reasons of power transmission. Similarly in parametric applications the inductance of the device must be produced mainly by the film itself and as little as possible by stray inductance in order to obtain a sufficient amount of nonlinearity. The simplest coupling consists of a coil wound around the film. However, this configuration leaves a considerable air gap between the coil and the film. An alternate possibility is the deposition of a conductive film under and above the magnetic film thus forming a very close loop around the magnetic material.

3. Experimental Results

3.1 Measurements of materials

The requirements for the material to be used in a parametric device are repeated here in greater detail:

1. pronounced nonlinearity of the *B-H* characteristic (sharp 'knee", see Fig. 1)

2. low losses in the frequency range of interest for small signals as well as for large ones.

3. possibility of producing small and varied shapes (toroids, films).

The first requirement is obviously the basis for parametric operation. A sharp "knee" permits use of low pump amplitudes (and therefore power).

The second requirement has two aspects. For small signals, such as the input and output signals of a converter, a good Q is desirable to obtain good gain. For large signals, namely the pump, the losses as given by the area of the hysteresis curve should be low in order to save pump power.

The third requirement demands that the shape of the ferrite element must allow the application of the magnetic field with little stray inductance. Too much stray inductance tends to decrease the nonlinear properties of the element. Furthermore, the size of the element should permit parametric action at the power levels in question. An oversized element just wastes pump power and is not desirable from the point of view of miniaturization.

3.1.1 Ferrites

The tests performed on a number of materials (square loop, high frequency, high Q materials, etc.) indicate that it is difficult to achieve a pronounced nonlinearity and low losses at the same time. The materials tend to be nonlinear but lossy or lossless but linear. Furthermore the required qualities deteriorate with increasing frequency.

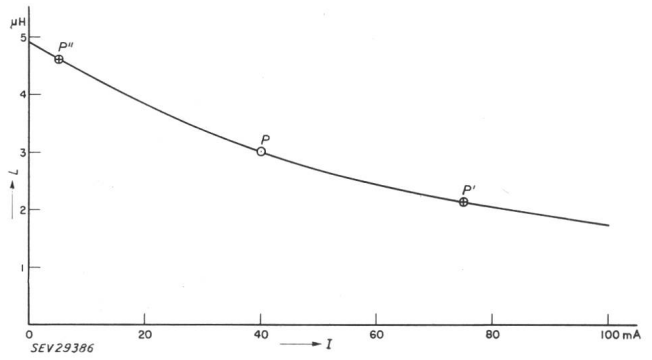

Fig. 5

Small-signal inductance L of Japanese "Parametron" core as a function of dc-bias I

Coil with10 turns

Fig. 5 shows the small signal inductance as a function of the bias of a ferrite core (as used in the Japanese parametron computer element). However, the Q of this material deteriorates considerably at frequencies above 3 Mc/s.

A material with $Q \approx 60$ up to 15 Mc/s has been developed in the Electronics Laboratory of General Electric Company. The inductance as a function of bias is shown in Fig. 6. As a consequence of the hysteresis loop, the function $L = L(I)$ consists of two branches. A plot of the small signal Q as a function of frequency is represented in Fig. 7.

A further test which gives some information on the behavior of the material in a circuit consists in producing subharmonic oscillations. The amplitude of oscillation as a function of pump power, frequency and the circuit used are shown in Fig. 8. It can be seen that the pump power necessary to produce a given oscillation amplitude increases as the frequency raised to a power greater than 1. Since the hysteresis losses are expected to increase linearly with frequency, this result indicates that additional losses become significant with increasing frequency.

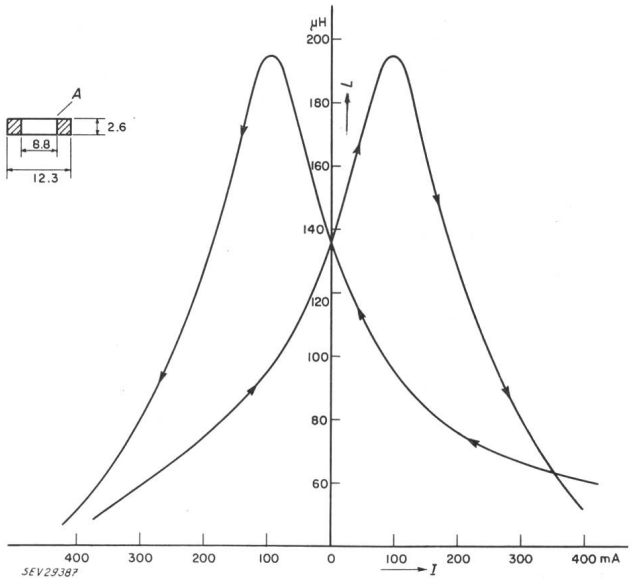

Fig. 6

Small-signal inductance as function of bias of experimental ferrite

A Dimensions of ferrite core [mm]; Coil with 100 turns

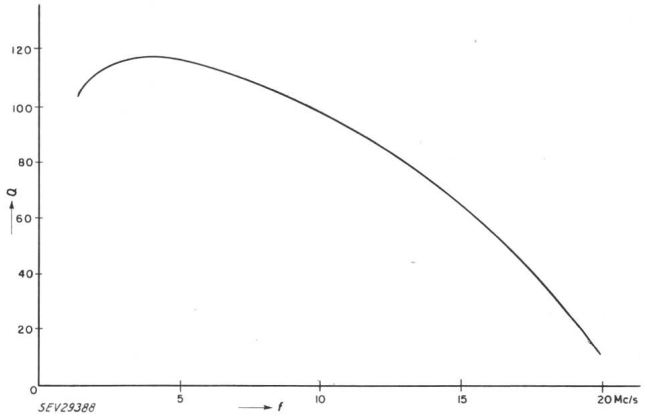

Fig. 7

Quality factor Q of experimental ferrite as a function of frequency f

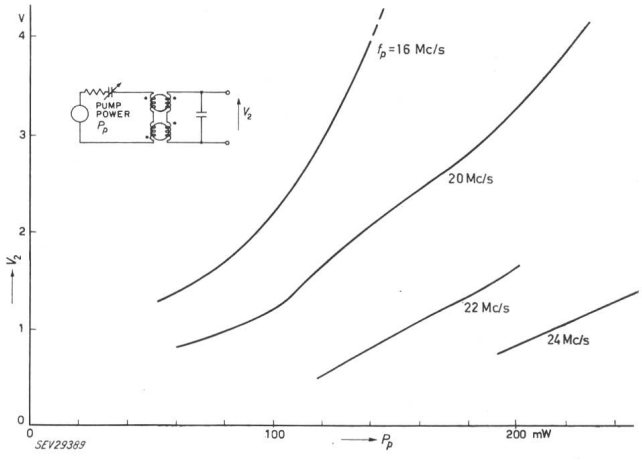

Fig. 8

Subharmonic oscillations produced with experimental ferrite cores

V_2 Amplitude of oscillations; P_p Pump power; f_p Pump frequency

The limit frequency for parametric operation of a material is not a well defined quantity but depends rather on how much pump power it is necessary to use. For the "Parametron" material, a practical figure is about 2 Mc/s, and for the material shown in Figs. 6, 7 and 8 about 10 Mc/s.

3.1.2 Magnetic films

The magnetic films in question are deposited on a thin glass plate (¼″ × ¼″ or 6 × 6 mm). The coil associated with the signal resonant circuit is wound directly on the film in order to minimize the air gap and to couple to the field perpendicular to the easy axis. The coil which introduces the pump power is perpendicular to the first one.

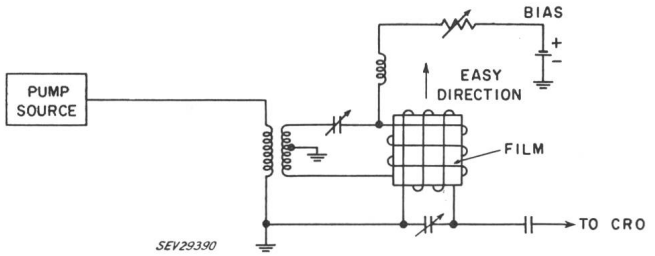

Fig. 9

Subharmonic oscillator using magnetic films

Signal coil 25 turns; pump coil 16 turns; film 1000 Å (10^{-4}) thick on glassplate ¼″ × ¼″ (6 × 6 mm)

Due to the short time available for the investigation, only a quick check of the subharmonic oscillation has been made as shown in Fig. 9. The pump power is fed to the film through an unbalanced-balanced transformer which reduces the interaction between pump and signal. Subharmonic oscillations up to 25 Mc/s (pump 50 Mc/s) haved been obtained. The pump power actually entering the film could not be measured due to undetermined losses in the transformer and through radiation. The amplitude of oscillation was in the order of 100 mV.

It is believed that the frequency of operation can be increased by using a shielded circuit configuration (for example, coaxial) with proper field concentration on the film and the proper choice of shape and size of the latter.

3.2 Measurements of circuits

3.2.1 Four core circuit

The test circuit is of the type shown in Fig. 3. "Parametron" cores are used which are biased to point P (Fig. 5). The total dc power consumption is in the order of 10 mW.

Operating the circuit as a *noninverting upconverter*, a stable theoretical maximum gain of $G = f_2/f_1$ is expected. Due to the losses in the material, a lower gain is obtained. Furthermore, the output signal shows some residual modulation (10–20%) at the input frequency. A reduction of this is a matter of balancing the core windings, etc., but this has not been carried out extensively.

The values of frequencies, gain and bandwidth are:

$f_1 = 0.38$ Mc/s, $f_2 = 2.48$ Mc/s, $f_0 = 2.1$ Mc/s
theoretical max. gain $G_{max} = f_2/f_1 = 6.5$ (8 db)
measured gain $G = 2.5$ (4 db)
overall bandwidth $B_{tot} = 80$ kc/s

The output of the *noninverting converter* as a function of pump voltage tends to a saturation value as shown in Fig. 10 curve *I*. Curve *II* shows the basically different behavior of the *inverting converter* tending towards the oscillatory

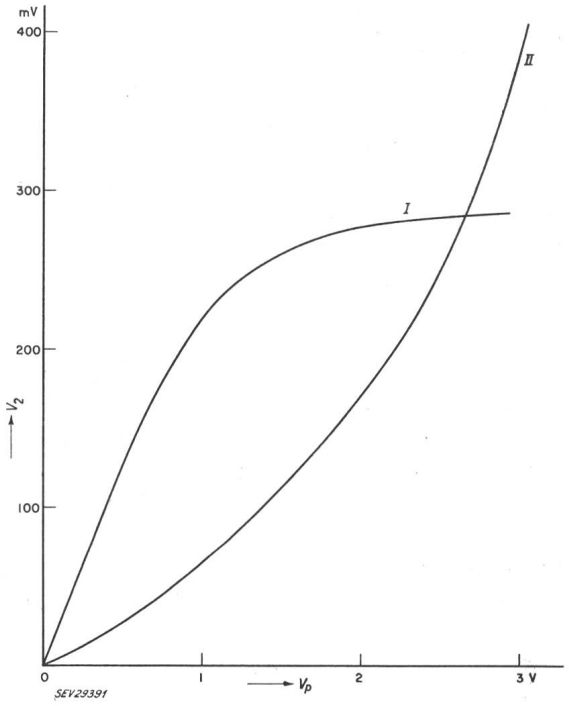

Fig. 10

Output voltage of parametric converter as a function of pump voltage

I Noninverting upconverter (19 mV input)
II Inverting upconverter (3 mV input)

condition as the pump power is increased. The potential instability of the inverting converter is illustrated by the gain and bandwidth measurement in Fig. 11. As a result, as the pump power increases the gain increases towards in-

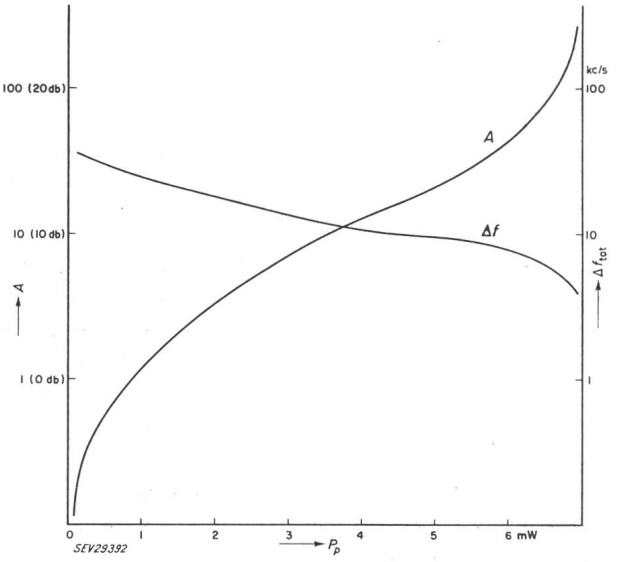

Fig. 11

Gain A and bandwidth Δf_{tot}. of inverting upconverter as a function of pump power P_p

finity (oscillation) and the bandwidth decreases towards zero. In the immediate neighborhood of this condition the circuit is very sensitive to changes of pump power and of

any other parameter. For stable operation the pump power must be reduced somewhat.

Since the inverting circuit shows a negative input resistance [Eq. (16)], it can be operated as an *amplifier* by removing the resistive load from the output circuit, which now becomes the idler circuit, and by extracting the output power from the input. The relationship between pump power, gain and bandwidth is essentially the same as for the inverting converter (Fig. 11).

The oscillating converter can be considered as a *two-frequency oscillator* which converts energy at the pump frequency f_0 to energy at the frequencies f_1 and f_2 and maintains the relationship $f_1 + f_2 = f_0$. An overall efficiency of about 10% has been measured.

As far as *noise* is concerned relative measurements have been taken on an inverting upconverter (the reason for this configuration is the high gain which overcomes the noise of the following amplifier). It has been found that the sensitivity of this circuit is about the same as that of a commercial receiver.

3.2.2 Bridge circuit

The circuit described in Section 2.2 and shown in Fig. 4 has been operated as an inverting converter up to a signal frequency of 8 Mc/s. The necessary pump power is very high (about 100 mW per core) especially in view of the small dimensions of the core [outer diameter 0.08″ (2 mm); inner diameter 0.05″ (1.2 mm); thickness 0.025″(0.6 mm)]. The separation between the different signals (input, output, pump) is satisfactory.

4. Conclusions

It can be seen from the literature that ferrites and probably magnetic films are considerably more resistant to nuclear radiation than diodes and transistors. Because of this fact, it is very attractive to use these materials as active elements in a parametric mode of operation, namely, as subharmonic oscillators, amplifiers and converters intended for use in such environments. It has been shown that parametric operation is possible using ferrite in the shape of toroidal cores and thin magnetic films. The associated circuit problems (separation of signals from each other) can be solved with a reasonable number of components. However, the problems concerning the material itself are more complex. In the case of ferrites for the time being it is difficult to build a material having low losses and pronounced nonlinearity in the HF range. In addition, the present knowledge of ferrite materials is not sufficient to determine which parameters in the composition of the ferrites produce the desired electrical characteristics. For the same reason any prediction on future development is extremely difficult. As a consequence, parametric operation using ferrites is practically limited to frequencies below 10 Mc/s. In order to handle a given amount of signal power the volume of ferrite involved, i. e. the size of the core, can be chosen within certain limits.

As far as magnetic films are concerned, there is reason for greater optimism regarding parametric operation at higher frequencies. For example, when used as bistable memory elements much shorter switching times have been obtained with films than with cores. A further advantage of films is that they can be produced in a considerable variety of shapes and can therefore be adapted to special physical structures (e. g. coaxial) which might be necessary at higher frequencies.

The main problem in the application of films seems to be the coupling between the fields in the film and the currents and voltages pertaining to the input and output circuitry. In order to obtain this coupling, a variety of structures is possible.

Appendix

7.1 *Parametric operation of nonlinear ferrite*

In the following a lossless ferrite material is assumed, having a nonlinear *B-H* characteristic as given by Eq. (1)

$$\Phi = \Phi(\Theta) \qquad (1)$$

Φ magnetic flux
Θ ampere turns

Putting

$$\begin{aligned} \Theta &= \Theta_b + \Theta_o + \Theta_s \\ \Theta_s &= \Theta_1 + \Theta_2 \\ \Theta_s &\ll \Theta_o \end{aligned} \qquad (2)$$

where the meaning of the subscripts is:

b bias	1 input
o pump	2 output
s signal	

Following standard techniques [3] $\Phi(\Theta)$ is developed in a Taylor series

$$\Phi(\Theta) = \Phi(\Theta_o + \Theta_b) + \frac{d\Phi}{d\Theta} \cdot \Theta_s + \ldots \qquad (3)$$

$$\begin{aligned} \Theta &= \Theta_b + \Theta_o \\ &= \Phi(\Theta_o + \Theta_b) + l(t) \cdot \Theta_s \end{aligned}$$

where

$$l(t) = l_o + 2l_1 \cos(\omega_o t) \qquad (4)$$

The time origin is now fixed since no phase constant is allowed in the second term. Differentiating with respect to time gives the voltage induced in one turn

$$\begin{aligned} x = \frac{d\Phi}{dt} &= l\frac{d\Theta_o}{dt} + \frac{d}{dt}(l\Theta_s) = l_o\frac{d\Theta_o}{dt} + \\ &+ 2l_1 \cos(\omega_o t)\frac{d\Theta_o}{dt} + (l_o + 2l_1 \cos\omega_o t)\frac{d\Theta_s}{dt} - \\ &- 2l_1\omega_o \sin(\omega_o t) \cdot \Theta_s \end{aligned} \qquad (5)$$

As can be seen from the right side of Eq. (5) the quantity x contains the frequencies f_o, $2f_o$, f_1, f_2, $f_o \pm f_1$ and $f_o \pm f_2$. At this point a certain relationship between the input and output frequency of the form $\pm f_1 \pm f_2 = f_o$ is forced by inserting ideal filters passing only the frequencies f_o, f_1 and f_2 into the respective circuit sections (see Fig. 12). All the real quantities are represented in the form

$$\Theta_1(t) = \Theta_1 e^{j\omega_1 t} + \Theta_1^* e^{-j\omega_1 t}$$

where the * denotes the complex conjugate quantity. By introducing all the quantities in Eq. (5) and by comparing coefficients carrying the same frequency the following is obtained:

for $\omega_2 = \omega_1 + \omega_o$ (noninverting converter)

$$\begin{pmatrix} x_1 \\ x_2 \end{pmatrix} = \begin{pmatrix} j\omega_1 l_o & j\omega_1 l_1 \\ j\omega_2 l_1 & j\omega_2 l_o \end{pmatrix} \begin{pmatrix} \Theta_1 \\ \Theta_2 \end{pmatrix} \tag{6}$$

for $\omega_o = \omega_1 + \omega_2$ (inverting converter)

$$\begin{pmatrix} x_1 \\ x_2^* \end{pmatrix} = \begin{pmatrix} j\omega_1 l_o & j\omega_1 l_1 \\ -j\omega_2 l_1 & -j\omega_2 l_o \end{pmatrix} \begin{pmatrix} \Theta_1 \\ \Theta_2^* \end{pmatrix} \tag{7}$$

The equations above describe the parametric device in terms of quantities associated with the material. In order to

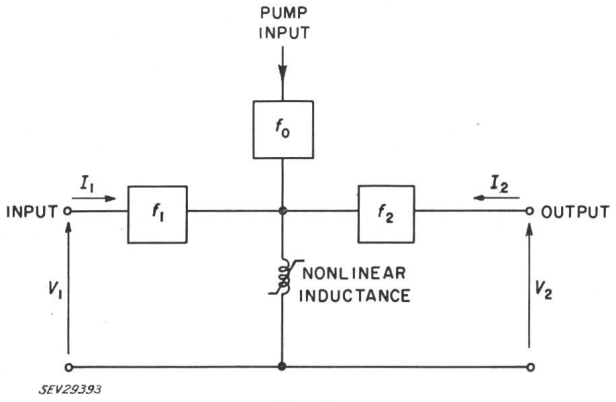

Fig. 12
Schematic of parametric circuit

obtain relationships between voltages and currents, a toroidal core is assumed with an input winding (N_1 turns) and an output winding (N_2 turns). The following relationships are considered to apply:

$$\begin{aligned} V_1 &= N_1 x_1 & V_2 &= N_2 x_2 \\ \Theta_1 &= N_1 I_1 & \Theta_2 &= N_2 I_2 \end{aligned} \tag{8}$$

a) Noninverting converter $\omega_1 + \omega_o = \omega_2$

Introducing Eq. (8) into Eq. (6) leads to

$$\begin{pmatrix} V_1 \\ V_2 \end{pmatrix} = \begin{pmatrix} j\omega_1 l_o N_1^2 & j\omega_1 l_1 N_1 N_2 \\ j\omega_2 l_1 N_1 N_2 & j\omega_2 l_o N_2^2 \end{pmatrix} \begin{pmatrix} I_1 \\ I_2 \end{pmatrix} \tag{9}$$

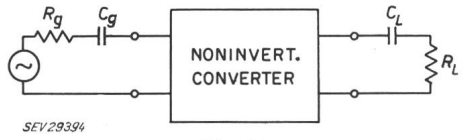

Fig. 13
Converter circuit connected to generator and load

The noninverting upconverter is connected to a generator and to a load as shown in Fig. (13). It is assumed that the input and output tuning perform as ideal filters. The gain is given by

$$G = \frac{\omega_2}{\omega_1} \cdot \frac{4\, r\, l'}{(r + l')^2} \tag{10}$$

where

$$\begin{aligned} r &= R_g R_L \\ l' &= \omega_1 \omega_2 l_1^2 N_1^2 N_2^2 \\ 1 &= \omega_1^2 l_o N_1^2 C_g \\ 1 &= \omega_2^2 l_o N_2^2 C_L \end{aligned}$$

For matched conditions ($r = l'$), the gain becomes maximum namely ω_2/ω_1, a well known result.

Furthermore, it may be seen that

$$Q_1 Q_2 = \frac{l_o^2}{4 l_1^2} \tag{11}$$

If the same bandwidth is prescribed for the input and output circuits

$$B = \frac{f_1}{Q_1} = \frac{f_2}{Q_2}$$

Under matched conditions B becomes

$$B = \frac{2 l_1}{l_o} \sqrt{f_1 f_2} \tag{12}$$

For the circuit using four cores (see Fig. 9) of which only two are driven by the pump, the above formulae are somewhat modified. The resonance conditions become

$$\begin{aligned} 1 &= 4\, \omega_1^2 l_o N_1^2 C_g \\ 1 &= 4\, \omega_2^2 l_o N_2^2 C_L \end{aligned} \tag{13}$$

and the matching condition

$$R_g R_L = 4\, \omega_1 \omega_2 l_1^2 N_1^2 N_2^2 \tag{14}$$

b) Inverting converter $\omega_1 + \omega_2 = \omega_o$

This circuit is potentially unstable due to the negative input (and output) resistances. If the output is loaded with the impedance

$$Z_2 = R_L + \frac{1}{j\omega C_L}$$

The input impedance becomes [4])

$$\begin{aligned} Z_{in} &= z_{11} - \frac{z_{12}\, z_{21}}{z_{22} + Z_2^*} = \\ &= j\omega_1 l_o N_1^2 - \frac{\omega_1 \omega_2 l_1^2 N_1^2 N_2^2}{-j\omega_2 l_o N_2^2 + R_L - \dfrac{1}{j\omega_2 C_L}} \end{aligned} \tag{15}$$

If the output is tuned to the frequency f_2 the input impedance becomes

$$Z_{in} = j\omega_1 l_o N_1^2 - \frac{\omega_1 \omega_2 l_1^2 N_1^2 N_2^2}{R_L} \tag{16}$$

The negative real part is responsible for the amplification of the input signal. The gain increases with increasing l_1 or, in other words, with increasing pump power.

7.2 Bridge-type parametric circuit

A circuit which gives—at least theoretically—a perfect separation of every signal from every other (input, output, pump) is shown in Fig. 14. The circuit is a bridge and consists of four impedances $Z_1 \ldots Z_4$ which are related as follows [5])

$$\begin{aligned} Z_1 &= Z_2 = j\omega\, [L_o + 2L_1 \cos \omega_o t] \\ Z_3 &= Z_4 = j\omega\, [L_o - 2L_1 \cos \omega_o t] \end{aligned} \tag{17}$$

where L_o is the constant part of the inductance given by the dc bias and L_1 is caused by the pump.

The Z-matrix of the bridge circuit is given by:

$$(Z) = \frac{1}{Z_1 + Z_2 + Z_3 + Z_4} \times \begin{pmatrix} (Z_1 + Z_3)(Z_2 + Z_4) \,;\, Z_3 Z_4 - Z_1 Z_2 \\ Z_3 Z_4 - Z_1 Z_2 \,;\, (Z_2 + Z_3)(Z_1 + Z_4) \end{pmatrix} \tag{18}$$

---

[4]) Since in the inverting case the four-pole equations are written in terms of V_2^* and I_2^*, a physical impedance Z_2 must be introduced as Z_2^* in the equations, because $V_2^* = -Z_2^* I_2^*$.

[5]) The author is aware that in the following treatment quantities belonging to the time domain and to the frequency domain are mixed together, a procedure which generally is not permissable. However, the result will be the same as that obtained by treatment with the differential equation of the system. The more "intuitive" approach is shown because it gives better insight into the problem.

By introducing $Z_1 \ldots Z_4$ from Eq. (17) the following is obtained:

$$\left.\begin{aligned} &Z_1 + Z_2 + Z_3 + Z_4 = 4\mathrm{j}\omega L_o \\ &Z_1 + Z_3 = Z_2 + Z_4 = Z_2 + Z_3 = Z_1 + Z_4 = 2\mathrm{j}\omega L_o \\ &Z_3 Z_4 - Z_1 Z_2 = (\mathrm{j}\omega)^2 (-8 L_1 L_o \cos \omega_o t) \end{aligned}\right\} \quad (19)$$

and the matrix elements:

$$\left.\begin{aligned} z_{11} &= z_{22} = \mathrm{j}\omega L_o \\ z_{12} &= z_{21} = -2\mathrm{j}\omega L_1 \cos \omega_o t \end{aligned}\right\} \quad (20)$$

Writing the complete four-pole equations

$$\begin{aligned} V_1 &= z_{11} I_1 + z_{12} I_2 \\ V_2 &= z_{21} I_1 + z_{22} I_2 \end{aligned} \quad (21)$$

and assuming for example

$$\omega_2 = \omega_o + \omega_1$$

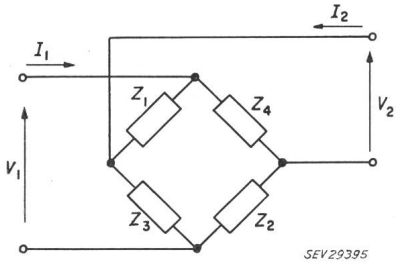

Fig. 14

Bridge-type parametric circuit

it may be seen that the term $z_{12}\ (\omega_o)\ I_2\ (\omega_2)$ represents a contribution to the voltage $V_1(\omega_1)$. If the current i_2 is allowed to assume the form:

$$i_2 = I_2' \cos \omega_2 t + I_2'' \sin \omega_2 t$$

the trigonometric products arising in Eq. (21) can be written as:

$$\cos \omega_2 t \cdot \cos \omega_o t = \frac{1}{2} \cos (\omega_2 - \omega_o) + \ldots$$

$$\sin \omega_2 t \cdot \cos \omega_o t = \frac{1}{2} \sin \underbrace{(\omega_2 - \omega_o)}_{= \omega_1} + \ldots$$

Therefore the Z-matrix of the noninverting converter becomes:

$$(Z) = \begin{pmatrix} \mathrm{j}\omega_1 L_o & -\mathrm{j}\omega_1 L_1 \\ -\mathrm{j}\omega_2 L_1 & \mathrm{j}\omega_2 L_o \end{pmatrix} \quad (22)$$

The minus signs of the terms z_{12} and z_{21} do not represent a real difference between this matrix and the one shown previously in Eq. (6). By interchanging the output terminals, that is the signs of I_2 and V_2, the minus signs disappear.

7.3 Calculations of magnetic films

It is assumed that an external magnetic field is applied to the magnetic film. The magnetization vector M then includes an angle φ with the easy axis of magnetization (see Fig. 15).

The free magnetic energy E per volume can be written [4] as

$$E = k \sin^2 \varphi - H_{\parallel} M \cos \varphi - H_{\perp} M \sin \varphi \quad (23)$$

where the symbols are explained in Fig. 15. The position of the vector M will minimize the potential energy. Therefore the angle φ is determined by

$$\frac{\delta E}{\delta \varphi} = 0 \quad (24)$$

An exact solution of Eq. (24) is not possible and any higher order approximation leads to bulky expressions. Since exact quantitative information is not necessary, the consideration

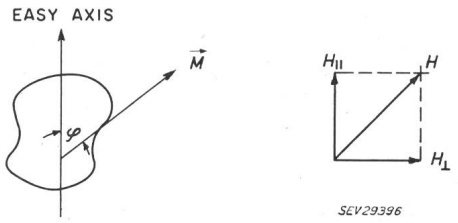

Fig. 15

Magnetic thin film under the influence of an applied magnetic field

M Magnetization vector; φ Angle; H Field-strength

is confined to small angles. This simplifies the calculation considerably but still allows an insight into the basic phenomenon. Thus, for small φ ($\sin\varphi \approx \varphi$; $\cos \varphi \approx 1$) the following expression is obtained:

$$\varphi = \frac{H_{\perp}}{\frac{2k}{M} + H_{\parallel}} = \frac{H_{\perp}}{H_k + H_{\parallel}} \quad (25)$$

$H_k = 2k/M$ is the so-called anisotropy field. Consider the magnetic induction B which is given by

$$\begin{aligned} B_{\parallel} &= \mu_0 H_{\parallel} + M \cos \varphi \\ B_{\perp} &= \mu_0 H_{\perp} + M \sin \varphi \end{aligned} \quad (26)$$

By introducing Eq. (25) into (26) the following is obtained:

$$\left.\begin{aligned} B_{\parallel} &= \mu_0 H_{\parallel} + M \left[1 - \frac{1}{2} \frac{H_{\perp}^2}{(H_k + H_{\parallel})^2}\right] \\ B_{\perp} &= \mu_0 H_{\perp} + M \frac{H_{\perp}}{H_k + H_{\parallel}} \end{aligned}\right\} \quad (27)$$

From the first equation (27) it can be seen that an ac magnetic field $H_{\perp} = H_0 \cos \omega t$ produces a flux density component $B_{\parallel}$ at the frequency 2ω through the relationship $\cos^2 \omega t = \frac{1}{2}(\cos 2\,\omega t + 1)$. This frequency doubling has been observed experimentally in the circuit of Fig. 9 by reversing the role of input and output. The small signal inductances can be derived by differentiation:

$$\left.\begin{aligned} \frac{\partial B_{\parallel}}{\partial H_{\parallel}} &= l_{\parallel} = \mu_0 + 2M \frac{H_{\perp}^2}{(H_k + H_{\parallel})^3} \\ \frac{\partial B_{\perp}}{\partial H_{\perp}} &= l_{\perp} = \mu_0 + \frac{M}{H_k + H_{\parallel}} \end{aligned}\right\} \quad (28)$$

It follows, for example, that the inductance l_l can be controlled by the field $H_{\parallel}$ thus making possible parametric operation. Since $H_{\parallel}$ and the field with l_l are perpendicular, and likewise the associated coils, the pump circuit and the actual signal circuit are decoupled.

Bibliography

[1] *Shelton, R. D.* and *J. G. Kenney:* Damaging Effects of Radiation on Electronic Components. Nucleonics Vol. 14(1956), No. 9, p. 66...69.

Author's address:

Dr. sc. techn. *A. Brändli*, Electronics Laboratory, General Electric Company, Syracuse, N. Y. (USA).